REPORT DOCUMENTATION PAGE

Form Approved
OMB No. 0704-0188

1. REPORT DATE *(DD-MM-YYYY)*	**2. REPORT TYPE**	**3. DATES COVERED** *(From - To)*
09-07-2010	Technical Paper	

4. TITLE AND SUBTITLE

Cold Flow Diluent Mixing Study Using Radial High Density Ratio Jets into a Circular Freestream

5a. CONTRACT NUMBER
FA9300-06-D-0003

5b. GRANT NUMBER

5c. PROGRAM ELEMENT NUMBER

6. AUTHOR(S)
Anh-Tuan Le & Ian Donovan (Advatech Pacific); Nils Sedano & Robert Bernstein (AFRL/RZSE)

5d. PROJECT NUMBER

5e. TASK NUMBER

5f. WORK UNIT NUMBER
33SP09AR

7. PERFORMING ORGANIZATION NAME(S) AND ADDRESS(ES)

Advatech Pacific
950 E. Palmdale Boulevard, Suite C
Palmdale CA 93550

8. PERFORMING ORGANIZATION REPORT NUMBER

AFRL-RZ-ED-TP-2010-321

9. SPONSORING / MONITORING AGENCY NAME(S) AND ADDRESS(ES)

Air Force Research Laboratory (AFMC)
AFRL/RZS
5 Pollux Drive
Edwards AFB CA 93524-7048

10. SPONSOR/MONITOR'S ACRONYM(S)

11. SPONSOR/MONITOR'S NUMBER(S)
AFRL-RZ-ED-TP-2010-321

12. DISTRIBUTION / AVAILABILITY STATEMENT

Approved for public release; distribution unlimited (PA #10334).

13. SUPPLEMENTARY NOTES
For presentation at the 46th AIAA/SME/SAE/ASEE Joint Propulsion Conference, Nashville, TN, 25-28 July 2010.

14. ABSTRACT

Project Themis is a recently created Air Force Research Laboratory (AFRL) research program that seeks to bridge the gap from lab-scale to full-scale testing and aid in developing engine technologies to a technology readiness level (TRL) of 4, so that they may be transitioned to current or future engine programs. Project Themis is named after the Greek goddess Themis, which means "law of nature". The goal is to research technologies associated with combustion devices using hydrocarbon fuel that support increased engine life, performance, and thrust-to-weight ratio. Preliminary literature search results show three areas that need further investigation. These are 1) the effect of injector type and chamber geometry on the main chamber performance and heat transfer, 2) the use of transpiration cooling for main chamber life, and 3) improvements on preburner temperature uniformity at the exit. Project Themis seeks to increase the understanding of impact of design variations in the diluent mixing at supercritical conditions especially in a 3D environment. The configuration of interest is jets injected transversely into a crossflow in a circular duct. Themis plans an experiment to study supercritical mixing in addition to the computational modeling efforts. The objective of the Advatech support effort is to use computational results to provide insight into the behavior of supercritical jets injected transversely into a crossflow in a circular duct.

15. SUBJECT TERMS

16. SECURITY CLASSIFICATION OF:			**17. LIMITATION OF ABSTRACT**	**18. NUMBER OF PAGES**	**19a. NAME OF RESPONSIBLE PERSON**
					Mr. Frank Friedl
a. REPORT	**b. ABSTRACT**	**c. THIS PAGE**			**19b. TELEPHONE NUMBER** *(include area code)*
Unclassified	**Unclassified**	**Unclassified**	SAR	19	N/A

Standard Form 298 (Rev. 8-98)
Prescribed by ANSI Std. 239.18

COLD FLOW DILUENT MIXING STUDY USING RADIAL HIGH DENSITY RATIO JETS INTO A CIRCULAR FREESTREAM

Anh-Tuan Le, Ian Donovan
Advatech Pacific, Incorporated
Redlands, CA

Nils Sedano, Robert Bernstein
Liquid Rocket Engines Branch (AFRL/RZSE)
Air Force Research Laboratory
Edwards AFB, CA

ABSTRACT

Project Themis is a recently created Air Force Research Laboratory (AFRL) research program that seeks to bridge the gap from lab-scale to full-scale testing and aid in developing engine technologies to a technology readiness level (TRL) of 4, so that they may be transitioned to current or future engine programs. Project Themis is named after the Greek goddess Themis, which means "law of nature". The goal is to research technologies associated with combustion devices using hydrocarbon fuel that support increased engine life, performance, and thrust-to-weight ratio. Preliminary literature search results show three areas that need further investigation. These are 1) the effect of injector type and chamber geometry on the main chamber performance and heat transfer, 2) the use of transpiration cooling for main chamber life, and 3) improvements on preburner temperature uniformity at the exit.

Project Themis seeks to increase the understanding of impact of design variations in the diluent mixing at supercritical conditions especially in a 3D environment. The configuration of interest is jets injected transversely into a crossflow in a circular duct. Themis plans an experiment to study supercritical mixing in addition to the computational modeling efforts.

The objective of the Advatech support effort is to use computational results to provide insight into the behavior of supercritical jets injected transversely into a crossflow in a circular duct.

Computational Fluid Dynamics (CFD) models of the experiment using Reynolds-averaged Navier-Stokes are employed to provide insight into the interaction between the injected and freestream fluids, as well as between the jets themselves. CFD simulations are also used to perform numerical experiments with variations of momentum flux ratios in support of design of the cold flow test apparatus.

Themis plans an experiment to study supercritical mixing in addition to the computational modeling efforts. The radial port geometry and arrangement are the principal design change that can be implemented to meet the temperature-mixing goals. The cold flow work will compare various configurations and their abilities to properly mix the diluent with the main flow stream. Configuration will begin with a single jet to validate the test results with the modeling tools and then moving to various port shapes and numbers.

INTRODUCTION

Project Themis is the Liquid Rocket Engines Branch (RZSE) in-house program that aims to address this capabilities gap, thereby providing for a multitude of research opportunities and a test bed for technology options. This effort seeks to continue the development of various technologies relevant to the combustion devices of liquid rocket engines from the lab-scale level and develop them to a level sufficient to be transitioned to industry or to other programs which support the Air Force needs. The technologies will be tested under various conditions from water

This work was performed under Contract FA9300-06-D-0003 0008 ETIP-A IPAT 9.0.

tests, to high pressure cryogenic inert fluids, up to the high pressure/ temperature/ heat flux combustion conditions that are relevant to modern, high performance rocket engines. As part of this incremental approach, a cold flow experiment is planned to research the area of interest (described below) in simulative environments while the hot fire facility is being built up. It will investigate the diluent mixing design, which is described as supercritical jets injected transversely into a crossflow in a circular duct. The in-House effort is focused on identifying and understanding underlying physics present in a configuration such as this. In order to better understand the underlying physics and better design experiments, computational modeling is being used in all aspects of the experiment.

Computational tools aid greatly in the analysis and design phases of experiments, when used in conjunction with available experimental data to guide modeling assumptions and generate accurate results. The objective of this study is to use results from computational tools to support the design of the test hardware, development of the test plan, and supplement the experimental data by providing insight into the and interaction between the injected and freestream fluids, as well as between the jets themselves. Validation of the CFD is accomplished by comparison with experimental visualization of water jet injection. Once validated, the same modeling approach is employed to provide information on the behavior of transverse jets at supercritical conditions.

This paper coincides with experimental work published by Sedano, *et al.*[5], where a more detailed description of the experiment and overall goals is provided.

APPROACH

Cold-flow injection experiments are being designed at the Air Force Research Laboratory (AFRL) at Edwards Air Force Base. CFD models attempt to capture as accurately as possible the features of the experiment setup that affect the flow characteristics, at the same time conserving computational resources by omitting parts that are not expected to contribute immediately to the physics of interest (for example, injection fluid manifolds, or the nuts and bolts holding the apparatus together). Figure 1 illustrates the initial concept of the hardware setup of the cold flow experiment. The test apparatus has a long runup section (length/diameter ratio of 50) followed by the test section, wherein a manifold feeds a number of injection ports into the test section. .

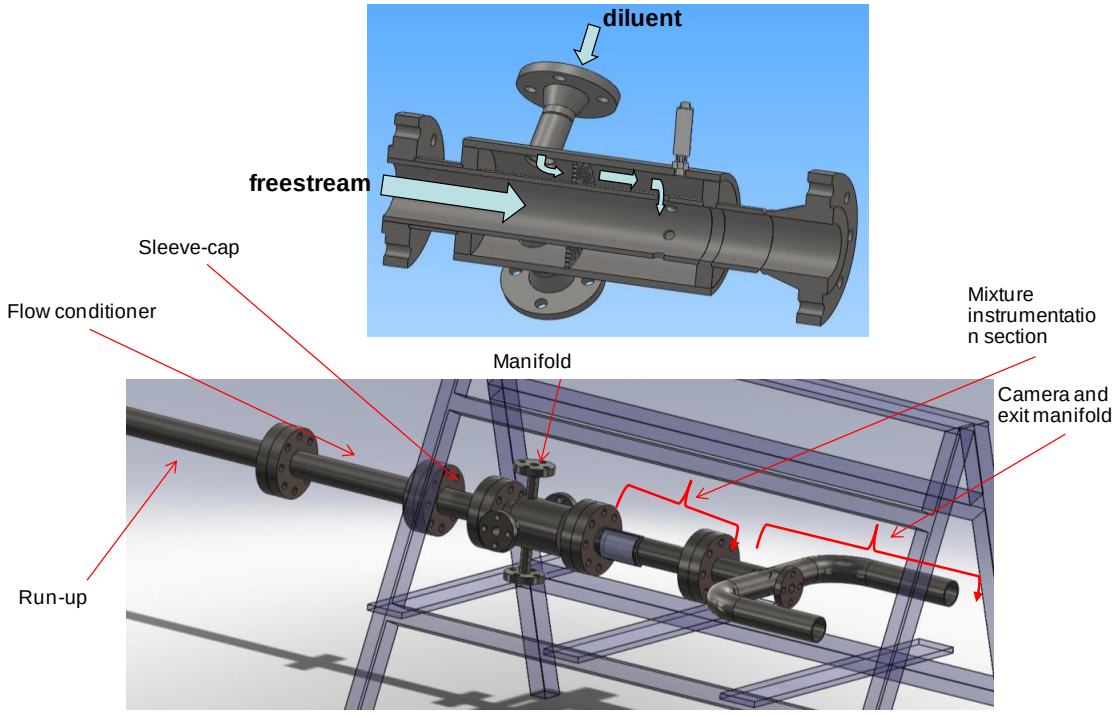

Figure 1: Geometry of Project Themis high-pressure injection test rig

The geometry for the flow models are simplifications of the test rig design, provided by AFRL as computer-aided design (CAD) solid models. From the CAD model, computational grids are generated for the CFD simulations using Gridgen v.15. Appropriate flow modeling parameters for each particular test case were chosen (these are described individually in the sections below), and flow simulations were performed with CFD++. The flow solutions were post-processed using Tecplot 360.

The CFD modeling approach is validated by comparing simulations of water jet injection with experimental visualization of the same flow. Once validated, the modeling approach is employed in the simulations for flows at supercritical conditions.

DISCUSSION

Three sets of simulations are performed:

1) Water jet experiments. This task is performed to validate CFD calculations against planar laser-induced fluorescence (PLIF) visualization results from water jet experiments performed for the Themis Project
2) Single jet cold flow. This task is performed to identify supercritical jet behavior in a bounded crossflow.
3) Dual jet cold flow. This task is performed to characterize jet interaction behavior at supercritical conditions.

The set up parameters and results from these cases are discussed in the sections below.

WATER JET SIMULATIONS

The geometry for the water jet simulations was provided by AFRL in a data file of International Geometry Exchange Standard (IGES) format, in which the inner mold line of the test section and injector is defined. The geometry consists of a cylindrical test section (2.067in diameter), with two transverse jet injectors (0.25in diameter) located on opposing sides of the test section (Figure 2).

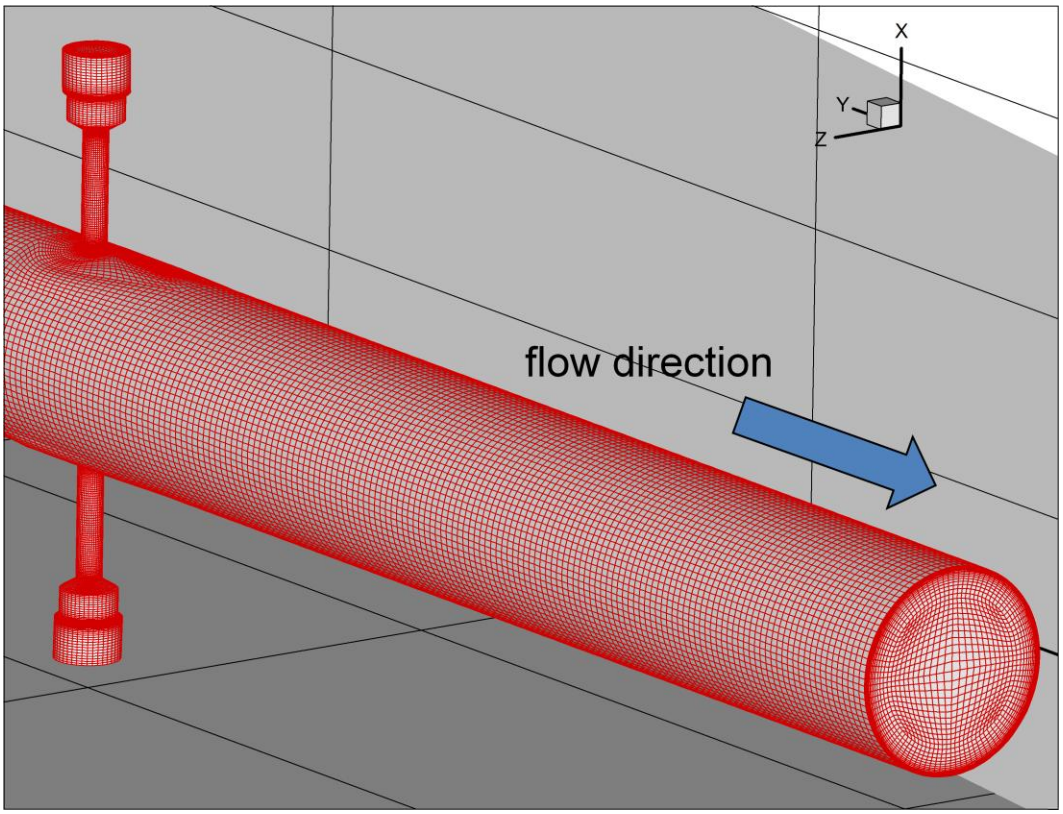

Figure 2: Geometry and Mesh Boundaries in Water Jet Simulations

Grid Generation and Flow Model

GRIDGEN v.15 was used to generate the volume mesh (Figure 2). The modeled domain contains 877 thousand hexahedral cells. Meshing is clustered near solid wall boundaries to capture the viscous boundary layer. As specified in the provided IGES geometry, the Cartesian coordinate system has the x-coordinate aligned with the injector axis, the y-coordinate aligned with the test section axis (freestream flow is in the negative-y direction), and the z-coordinate in the spanwise direction. The run-up to the test section was extended 5 diameters to allow the flow into the test section to be fully developed.

The flow conditions for the water jet simulations are shown in Table 1. The same injector is used for all the test cases; the velocity at the injector inflow is varied to obtain the desired momentum flux ratios.

Table 1: Flow Parameters for Water Jet Simulations

		Freestream	Diluent (single jet)
Fluid Parameters	Species	H_2O (l)	H_2O (l)
	Temperature (°K)	293	293
	Pressure (kPa)	101.3	101.3
	Density (kg/m^3)	999	999
Simulation #1	Velocity (m/s)	1.861	0.79
	J (momentum flux ratio)	5	

Simulation #2	**Velocity (m/s)**	**1.861**	**1.369**
	J (momentum flux ratio)	15	
Simulation #3	**Velocity (m/s)**	**1.861**	**1.936**
	J (momentum flux ratio)	30	
Simulation #4	**Velocity (m/s)**	**1.861**	**2.5**
	J (momentum flux ratio)	50	

The flow model parameters employed for this simulation are as follows:

- Incompressible Reynolds-averaged Navier-Stokes (RANS) governing equations
- Realizeable k-ε turbulence model with advanced two-layer wall function
- Liquid Law for viscosity and thermal conductivity
- Three fluid species, all with properties of liquid H2O (in order to distinguish between sources)

Boundary conditions in the simulation are applied as follows:

- Test section inflow with specified mass flow rate and temperature
  - $\dot{m}$ = 0.7645 kg/s, Tin=293^{o}K
  - CFD++ default turbulence intensity (2% freestream turbulence level)
- Injector inflows with specified mass flow rate and temperature
  - J=5: = 0.0250 kg/s, Tin=293^{o}K
  - J=15: = 0.0433 kg/s, Tin=293^{o}K
  - J=30: = 0.0613 kg/s, Tin=293^{o}K
  - J=50: = 0.0791 kg/s, Tin=293^{o}K
  - CFD++ default turbulence intensity (2% freestream turbulence level)
- Simple back pressure at test section exit
  - p=101.325 kPa (1 atm)
- Adiabatic (zero heat flux) no-slip walls at solid boundaries

Results

First, steady-state CFD calculations of the water visualization experiments were performed. All steady-state calculations were run for 3000 iterations, taking approximately 18 hours on 8 processors. The momentum ratio (J) of 15 was run first and its results were used as the initial condition for the other 3 cases. Subsequently, time-accurate calculations were run and video files generated to capture time-dependent behavior of the flow.

In Figure 3, isocontours of the diluents mass fraction at the symmetry plane in the time-accurate solutions are cast in the colors that match the experimental visualization to facilitate qualitative comparison. The jet penetration, jet interaction, and wake mixing characteristics from the simulations have similar features to the experiment. The primary flow mass fractions at the symmetry plane are plotted in Figure 3. The jets interact strongly at J= 30 and J=50, mildly at J=15, and only in the downstream wake region for J=5. Except for the J=5 case, where the computed flow is virtually steady, these plots also indicate that the CFD solutions capture the complex time-dependent flow

features resulting from the interaction of the jets at higher momentum flux ratios. The jet interactions result in wake regions that have distinct shapes, as well as different oscillatory and mixing behavior.

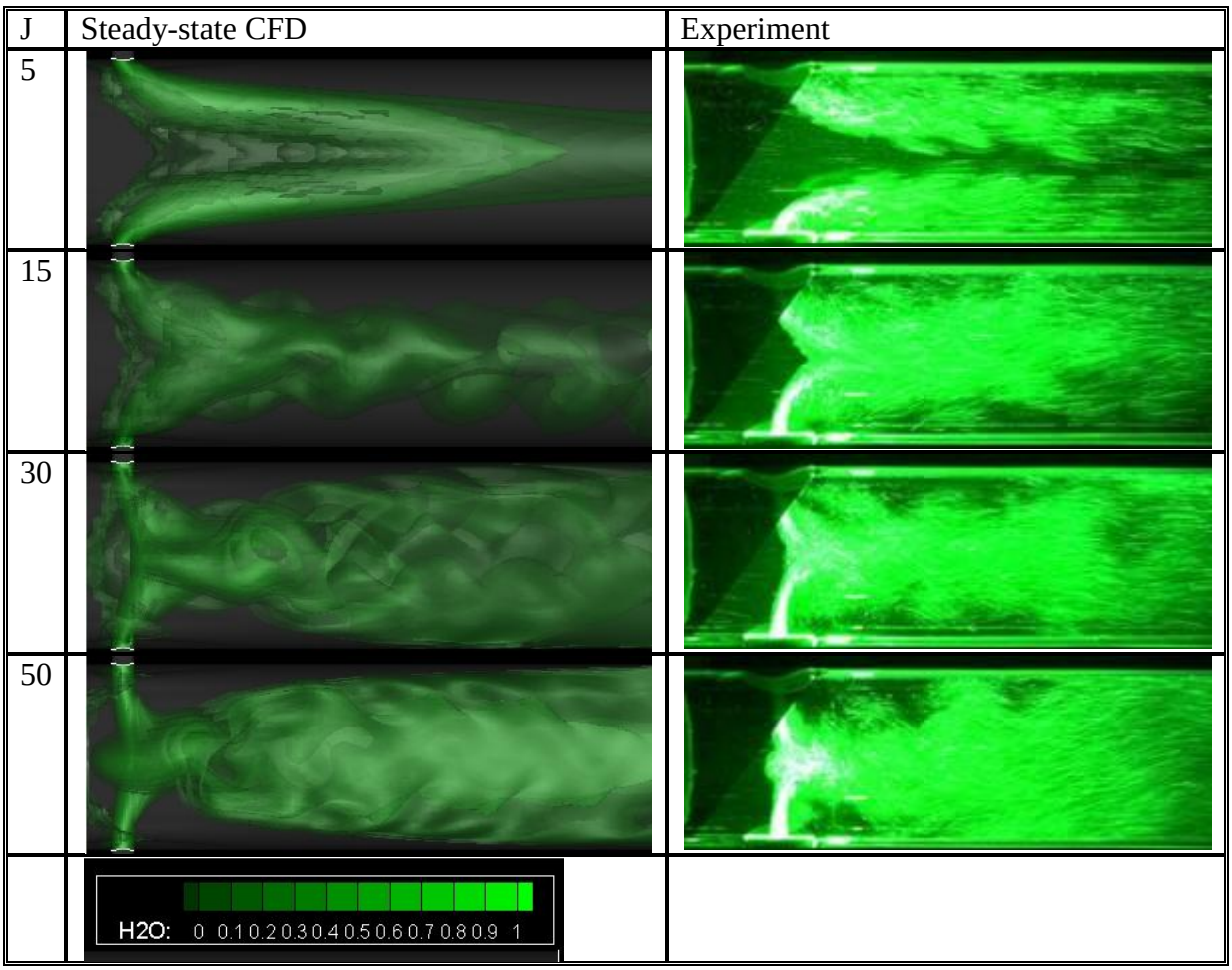

Figure 3: Primary Flow Mass Fraction Iso-surfaces in Steady-State Water Jet Simulations, in Comparison Against PLIF Visualization

One challenge that manifested itself from the time-accurate water jet simulations was that the unsteadiness in the calculated flows can be affected by the initial condition. One example is the J=30 case, in which the solution from the corresponding steady-state solution initiating was used as the initial conditions, resulted in a flow in which the fluctuations subsided to a steady condition. However, when the time-accurate calculation was initiated from another steady-state solution (J=15) the fluctuations in the calculated flow is sustained. The J=5 simulation also resulted in a relatively steady solution, where the experiment shows fluctuations in the wake region of the jet.

COLD FLOW SIMULATIONS

The cold flow simulations were completed to provide a guideline for investigation of the relevant modeling parameters for typical flow conditions inside the Themis high-pressure injection test rig. The baseline geometry was provided by AFRL in a data file of IGES format, in which the inner mold line of the test section and injector is defined. The injector manifold and exit manifold are not included in this model.

Grid Generation and Flow Model

Volume grids were generated using GRIDGEN v.15. Figure 4 shows the computational domain for the dual-jet configuration. The modeled domain contains 1.3 to 1.8 million hexahedral cells, depending on the number and size of the injectors. Meshing is clustered near solid walls to capture the viscous boundary layer, and near the injection point to capture high shear areas. In all simulations performed in this effort, the Cartesian coordinate system has the x-coordinate aligned with the test section axis, the y-coordinate aligned with the injector axis, and the z-coordinate in the spanwise direction.

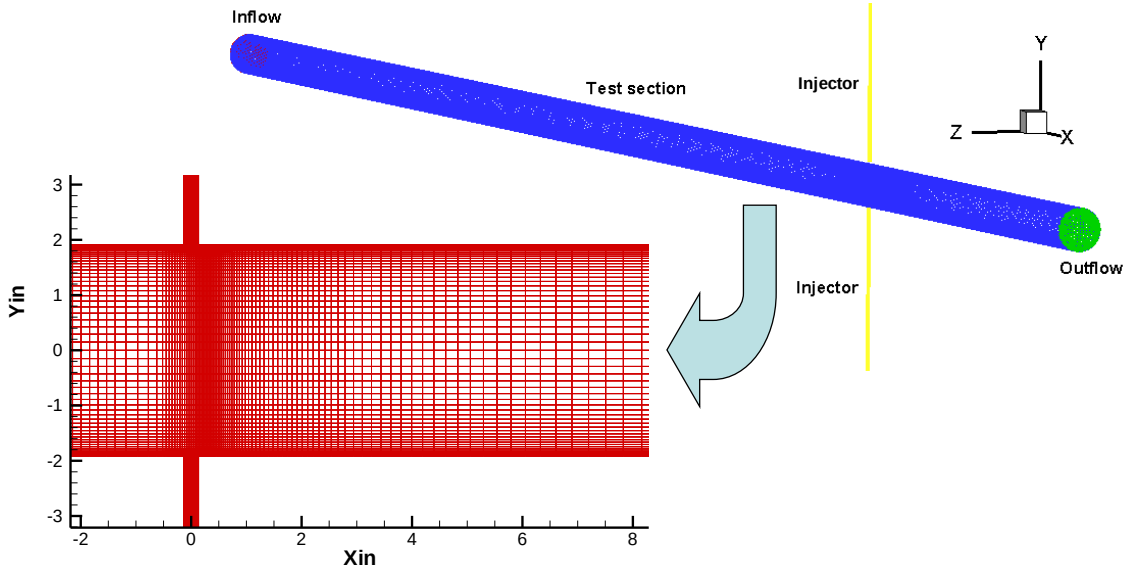

Figure 4: Grid for simulation of cold flow test rig (dual jet)

Flow conditions for the simulations are shown in Table 2. These are converted into SI units before implementation in the CFD model, since the Redlich-Kwong-Soave (RKS) equation of state used to model the supercritical fluids in CFD++ only accommodated fluid properties in SI units. Note that the mass flow rate remains constant for three injector sizes, resulting in lower jet velocities (and consequently, lower momentum ratios) as the injector diameter increases.

Table 2: Flow Parameters for Cold Flow CFD Simulations

		Freestream	Diluent (single jet)
Fluid Parameters	**Species**	**He/Argon Mix**	**N_2**
	Temperature (°R)	**535**	**150**
	Pressure (psi)	**1000**	**1000**
	Density (lbm/ft^3)	**1.09**	**49.8**
	Viscosity (lbm/ft-s)	**1.5000E-05**	**9.6884E-05**
	Mass flow rate (lbm/s)	**4.392**	**1.15**
Simulation #1 1/8" Sch 40 Injector	**Velocity (ft/s)**	**50.47**	**58.51**
	q (momentum flux ratio)	61.41	
Simulation #2	**Velocity (ft/s)**	**50.47**	**31.95**

1/4" Sch 40 Injector	**q (momentum flux ratio)**	18.32	
Simulation #3	**Velocity (ft/s)**	**50.47**	**17.42**
3/8" Sch 40 Injector	**q (momentum flux ratio)**	5.44	

The flow model parameters employed for this simulation are as follows:

- Compressible Reynolds-averaged Navier-Stokes (RANS) governing equations
- Redlich-Kwong-Soave (RKS) equation of state for non-ideal gases[4]
- Ideal gas equation of state (for debugging purposes)[1]
- Menter's Shear Stress Tensor (SST) turbulence model with advanced two-layer wall function[2]
- Sutherland's Law for viscosity and thermal conductivity
- Three fluid species with no reactions (helium, argon and nitrogen)

Boundary conditions are applied as follows:

- Subsonic test section inflow with specified mass flow rate and temperature
  - $\dot{m}$ = 1.992kg/s (4.392 lbm/s), T_{in}=297.2^{o}K (535^{o}R)
  - CFD++ default turbulence intensity (2% freestream turbulence level)
- Subsonic injector inflow with specified mass flow rate and temperature
  - $\dot{m}$ = 0.5216 kg/s (1.15 lbm/s), T_{in}=83.33^{o}K (150^{o}R)
  - CFD++ default turbulence intensity (2% freestream turbulence level)
- Simple back pressure at test section exit
  - p=144,000 slugs/ft-s2 (1000 psia)
- Adiabatic (zero heat flux) no-slip walls at solid boundaries

Results – Single Injector

First, single-injector simulations are performed to characterize the behavior of a jet into a bounded freestream. These calculations also provide a simple baseline to uncover technical issues in modeling the supercritical fluids.

Steady-state solutions were initially generated to provide a baseline visualization of the flow features. From fluctuations observed in the jet profiles, as well as numerical residuals from the solution, it was apparent that these flows are unsteady in nature. Consequently, time-accurate solutions are generated to resolve transient fluctuations in the flowfields in the study. Figure 5 shows the mass fraction distribution of helium (one constituent of the freestream fluid) at one instance in the time-accurate calculations, at the symmetry plane and cross-sections at several locations downstream of the injection point (marked by the white lines in the symmetry plane view). The diluent jet impinges strongly on the opposite wall, breaking up the coherence in the jet stream and induces large scale fluctuations in the fluid properties downstream of the injection point.

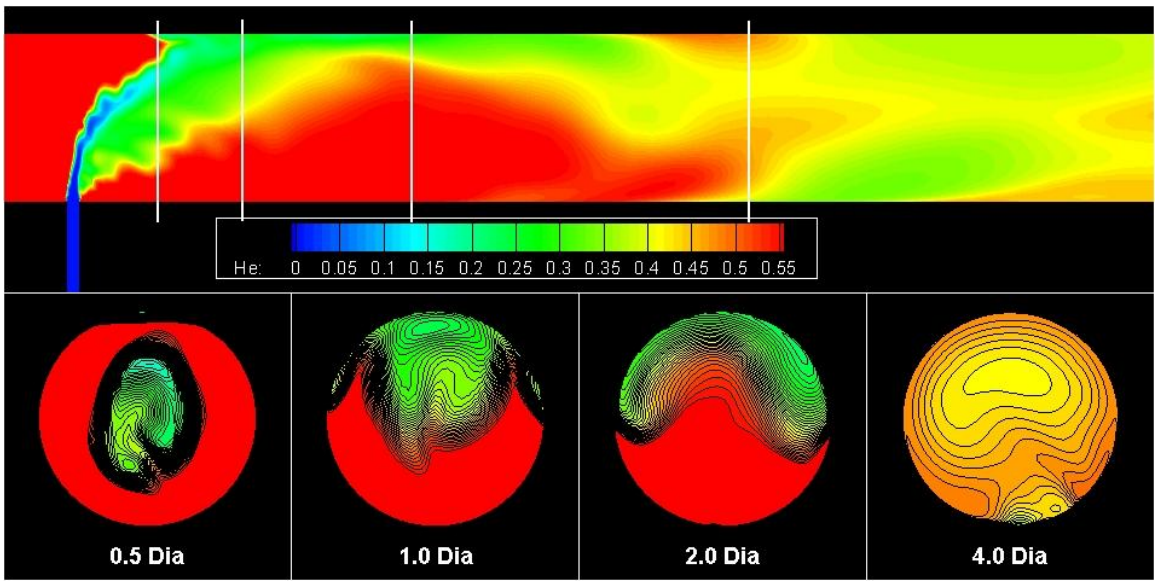

Figure 5: Helium mass fraction in Simulation #1 (1/8" Schedule 40 Pipe)

Temperature profiles of the same flow (in Figure 6) look nearly identical to the helium mass fraction. In the absence of chemical reactions, or a high level of compressibility, temperature behavior approximates that of a passive scalar. Hence, temperature can be used as a more easily measureable property to quantify the amount of mixing in these flows. Moreoever, since temperature behaves approximately like constituent mass fractions, and the latter provides a more direct characterization of flow uniformity, subsequent discussions will only include mass fraction.

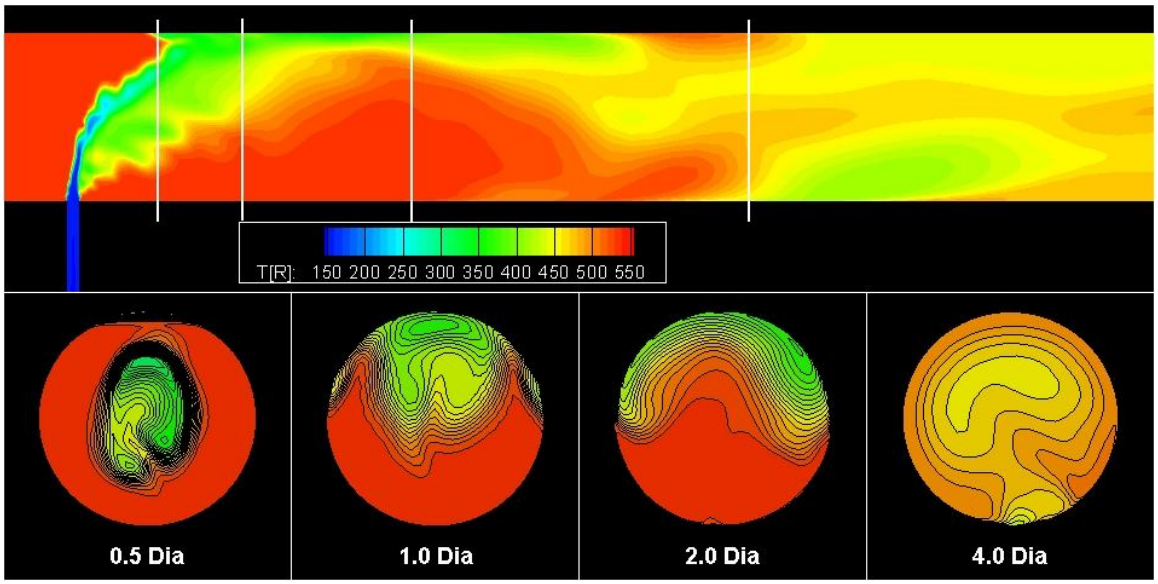

Figure 6: Temperature in Simulation #1 (1/8" Schedule 40 injector)

In Simulation #2, the jet is turned by the primary flow before impinging on the opposite wall approximately 4 test section diameters downstream (see Figure 7). There are significant fluctuations in the jet stream as it interacts with the primary flow, but it stays coherent much longer than in Simulation #1, where the jet impinges upon the opposite wall.

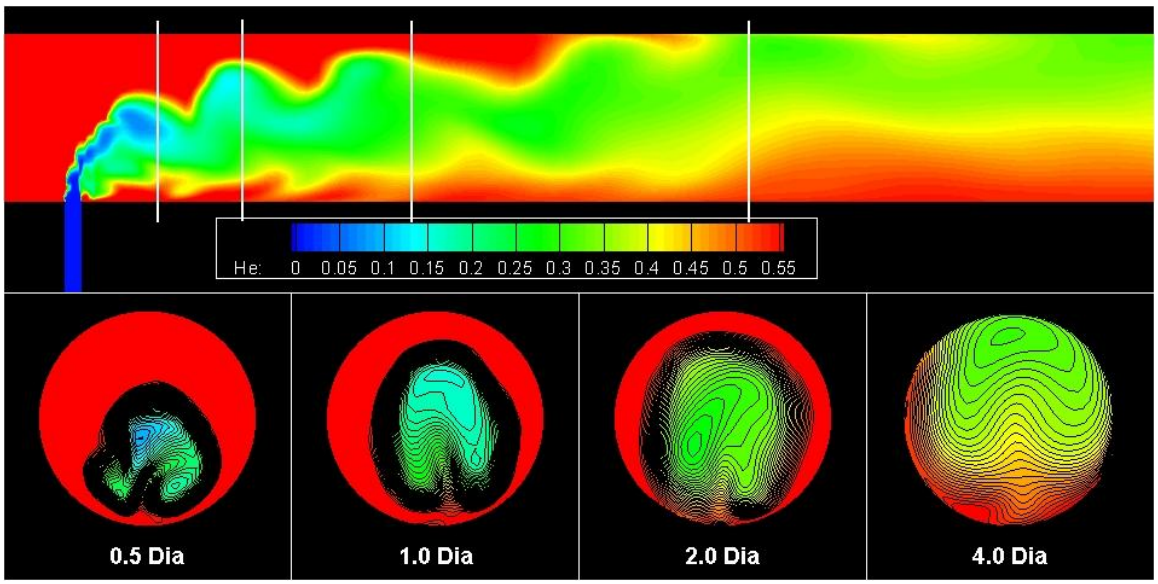

Figure 7: Helium mass fraction in Simulation #2 (1/4" Schedule 40 injector)

In Simulation #3, the jet is turned by the primary flow. The diluents jet does not impinge on the opposite wall until the jet expands far downstream. Fluctuations in the jet stream are small, so the jet stays coherent much longer than in Simulations #1 and #2.

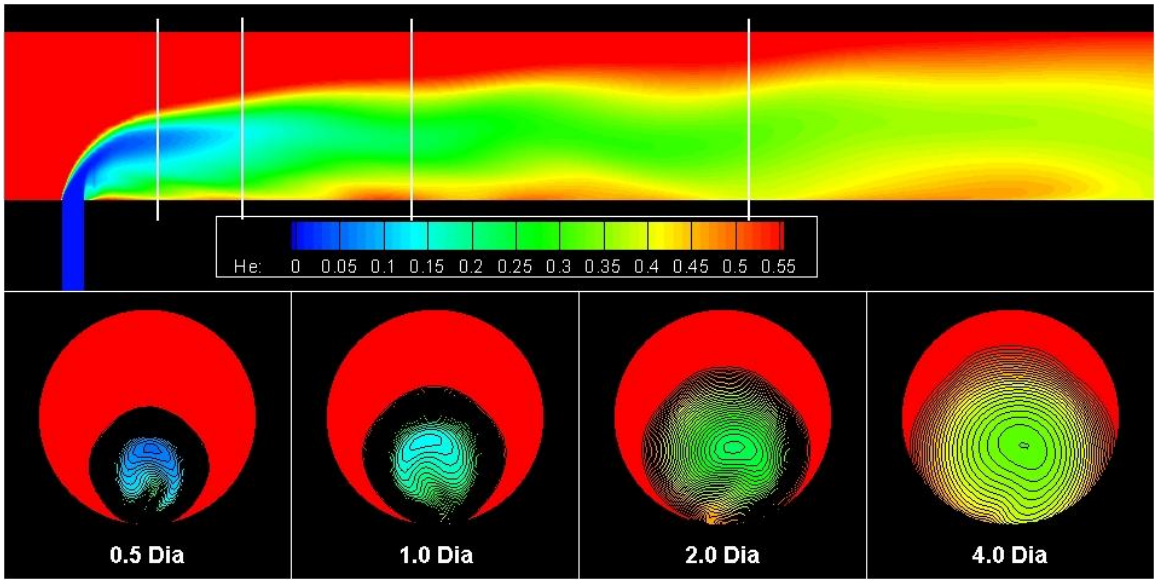

Figure 8: Helium mass fraction in Simulation #3 (3/8" Schedule 40 injector)

Results – Dual Injector

Subsequently, dual-injector simulations are performed to characterize the interaction of opposing jets in a bounded freestream. The geometry of the test section is the same as the single-jet case, with another injector of the same dimensions added on the opposite side of the test section wall. The flow conditions through the inflow boundaries for the simulations are the same as the single injector case (see Table 2). Thus, the mass flow rate for each injector (4.392 lbm/s) is kept the same as the single-injector simulation. Hence, the momentum flux ratio is the same as the single-injector simulations, but the total diluent mass and momentum flow are doubled. As in the single-injector cases, three injectors of different inner diameters are used to generate jets of different momentum fluxes with the same diluents mass flow rate.

Flow model parameters and boundary conditions are the same as in the single injector.

Steady-state CFD calculations of these flows are run for 7000-11000 iterations, requiring approximately 130-200 hours on 8 processors. Next, time-accurate calculations are run for 9000 iterations, taking approximately 180 hours on 8 processors. Along with the contour plots shown below, video files are generated to capture the time-dependent behavior of the flow.

Figures 9-11 shows the mass fraction distribution of helium (one constituent of the freestream fluid) at one instance in the time-accurate calculations, at the symmetry plane and cross-sections at several locations downstream of the injection point (marked by the white lines in the symmetry plane view). The Figures reveal the highly fluctuating behavior of the jet interaction. Note that the He mass fraction in Simulation #1 appears to be nearly uniform by four test section diameter downstream of the injectors (Figure 9), while in Simulations #2 and #3 (Figures 10 and 11, respectively) it doesn't appear fully uniform in Simulations #2 and #3 within this view of the test section (approximately 6 test section diameters).

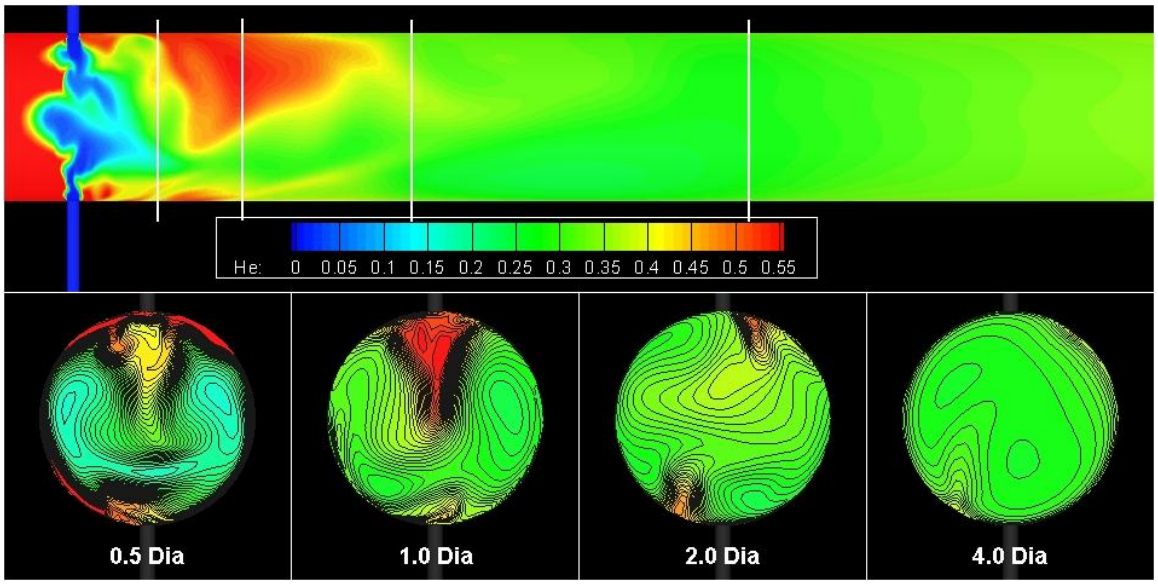

Figure 9: Helium Mass Fraction in Planar Slices of Dual-Jet Cold Flow Simulation #1

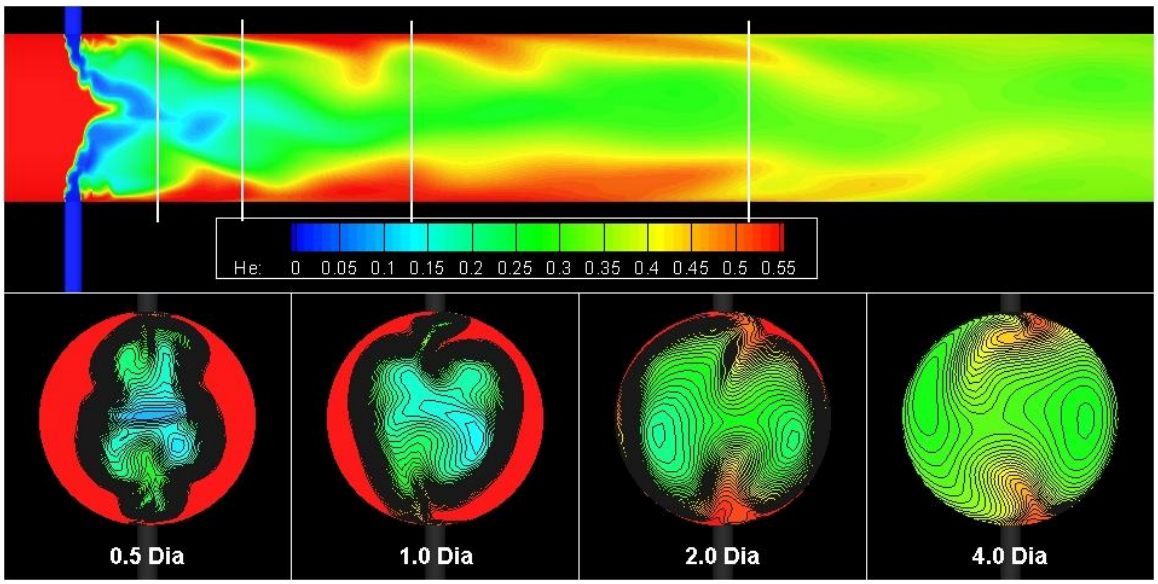

Figure 10: Helium Mass Fraction in Planar Slices of Dual-Jet Cold Flow Simulation #2

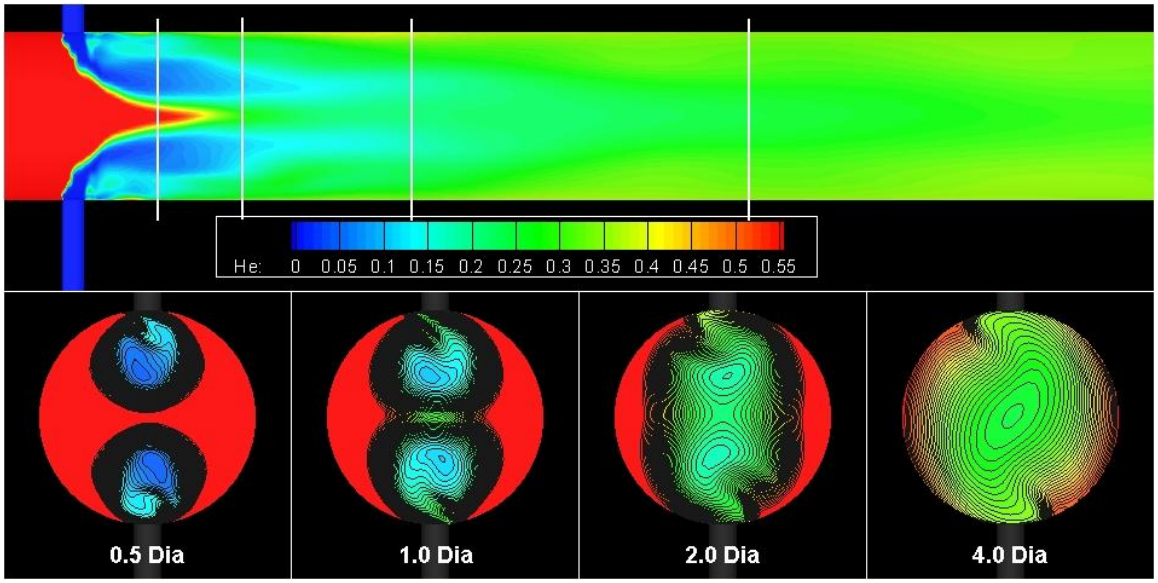

Figure 11: Helium Mass Fraction in Planar Slices of Dual-Jet Cold Flow Simulation #3

To quantify the amount of mixing in the test section, average and standard deviation of flow properties are calculated for cross-sectional planes at regular intervals of the test section. The average and standard deviation can be weighted by the surface area of the cells, or on the mass flux through the cells. The following are the equations used to calculate the average and standard deviations of flow properties.

Area-Averaged Properties:

$$Cav = \frac{\sum C_i A_i}{\sum A_i}$$

$$Cstd = \sqrt{\frac{\sum \left[(C_i - Cav)^2 A_i \right]}{\sum A_i}}$$

where *C* is the quantity being examined, *A* is the area of cell, *Cav* is the surface-area weighted average of C, and *Cst* is the surface-area weighted standard deviation of C.

Mass-Flux Averaged Properties: $Cavmf = \frac{\sum C_i A_i \rho_i U_i}{\sum A_i \rho_i U_i}$

$$Cstdmf = \sqrt{\frac{\sum \left[(C_i - Cavmf)^2 A_i \rho_i U_i \right]}{\sum A_i \rho_i U_i}}$$

where ρ is the fluid density, U is the velocity perpendicular to planar surface, *Cavmf* is the mass-flux weighted average of C, and *Cst* is the mass-flux weighted standard deviation of C.

From the CFD++ solution files, cross-sections of at various axial locations are extracted, resulting in a 2D surface. The values of flow properties in these 2D cells (approximately 2000 in each plane) are integrated once to calculate their average, and then integrated again to calculate the standard deviation. Both area-averaged and mass-flux averaged properties are calculated. Because the results based on the surface-area and mass-flux weighting differ only slightly, only the mass-flux averaged curves are shown in the Figures 12-14 below. The standard deviation of the flow property at each x-station is normalized by the average property at that station.

Figures 12-14 are ensemble averages of statistics taken from 31 solutions taken over 6000 iterations. These sample solutions are taken 3000 time steps after the time-accurate solutions were initiated, but they may not be fully flushed of residual flow structures from the steady-state solutions that were used as initial conditions. Nevertheless, they demonstrate how these statistics can be used to evaluate the uniformity of flow properties.

Mass fraction averages can be used to verify the consistency of the solution. Ideally, in the wake region (after the diluents jets have been turned by the freestream) mass fraction averages should be relatively constant, and the value should be close to the specified mass fraction at the inflow boundaries. Simulation 12 shows the axial profile of mass-flux weighted planar average of He mass fraction in the test section. In these simulations, the specified mass fraction for He is 0.38. Figure 12 shows that the calculated mass fraction in the domain is 10% low for Simulation #1 (1/8" Schedule 40 injector), 15% low for Simulation #2 (1/4" Schedule 40 injector), and 1% low for Simulation #3 (3/8" Schedule 40 injector). Thus, mass conservation has not been adequately achieved with these solutions. Thus, the current results can be used for general qualitative characterization of these flows, but quantitative assessments can not be considered conclusive. A more rigorous investigation into the effect of grid quality and numerical parameters used in the simulations will shed more light on the source of the solution inconsistency.

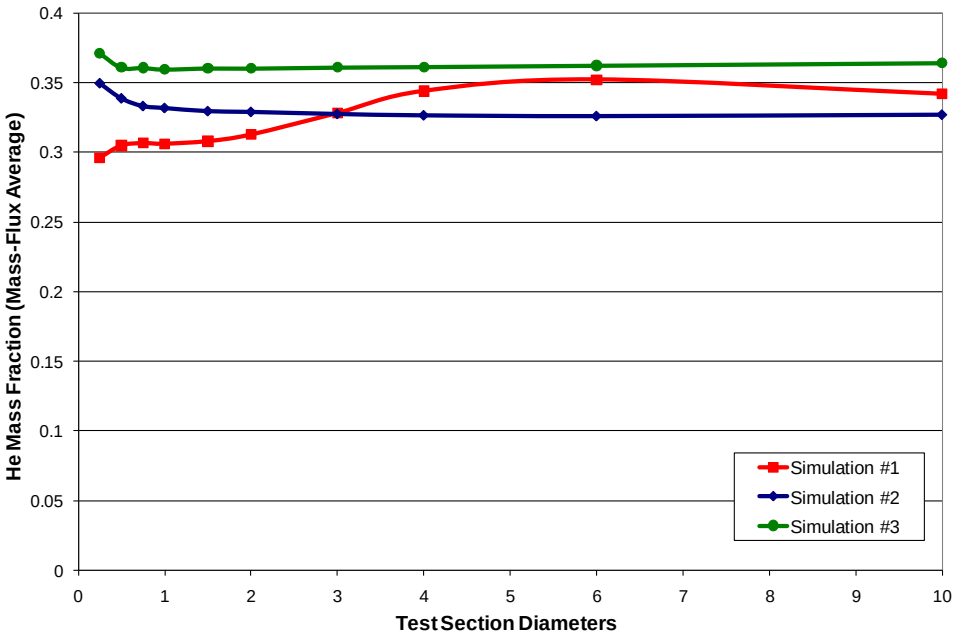

Figure 12: Mass-Flux Weighted Planar Average of Helium Mass Fraction

Standard deviations quantify the uniformity of a sample, and thus can be used to evaluate the relative degree of mixing in the domain. The more effective the mixing, the more uniform the distribution, and consequently the lower the standard deviation. Figure 13 shows that mixing is most effective with the highest momentum ratio (Simulation #1), since the standard deviation curve is the lowest in this case. It can also be surmised that the mixing may be of a different nature in Simulation #1 than in the other cases, since the curve is significantly different. The mass fraction contours in Figure 9 (above) shows that the diluent in Simulation #1 is has inter-jet mixing in front of (as well as behind) the injection point, where as the other cases (Figures 10 and 11) the jet interaction between the diluents jets (which enhance the fluctuations in the flow) take place after the injection point.

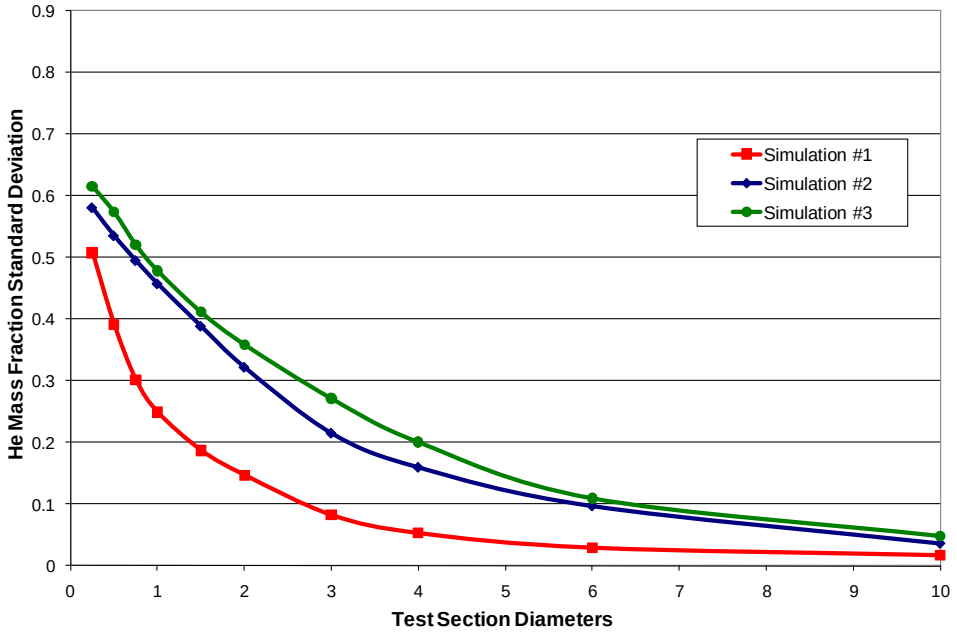

Figure 13: Mass-Flux Weighted Standard Deviation of Helium Mass Fraction

Figure 14 shows the standard deviation in the temperature distribution. As observed previously, temperature profiles show the same trends as the mass fraction. Thus, one could be used to assess the behavior of the other.

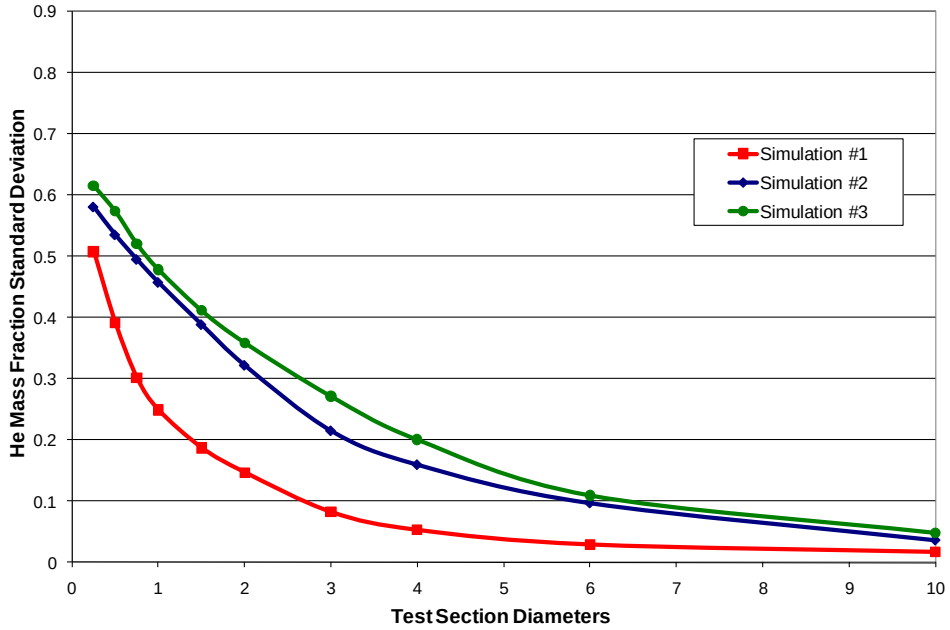

Figure 14: Mass-Flux Weighted Standard Deviation of Temperature

The high-pressure cold flow simulations present two major technical challenges. First, the calculated thermophysical properties of the diluent (N2) at the modeled temperature and pressure are significantly different from the fluids properties database at the National Institute of Standards and Technology (NIST). Secondly, numerical convergence is poor compared to those of the water jet simulations.

To investigate the calculated thermophysical properties, a comparison is performed between the fluid properties calculated by CFD++ with those from the National Institute of Standards and Technology (NIST) fluid properties database (Table 3). All calculated properties of the primary freestream constituent (He) are very similar to the NIST data. For the N_2 diluent, the density is within 3% of the NIST data (Table 3), suggesting that the RKS equation of state works adequately at the simulated condition, but the thermodynamic properties are significantly different (up to 70%), which suggests the calculated heat transfer and mixing behavior may not be accurate. One possible reason for the discrepancies in gamma (ratio of specific heats) for N_2 (and not He) is that the reference from which the coefficients in the CFD++ database are obtained[3] states that their data limit is 300^{o}K, whereas CFD++ extends the curve fit down to 100K (recall our calculation for N_2 is at 83.3^{o}K, and He is 297^{o}K). The other reason may be that the simulated condition is simply closer to the critical point for N_2, where existing physical models tend to break down.

Table 3: Differences between CFD++ and NIST Data

		Freestream	Diluent (single jet)
Fluid Parameters	Species	He	N_2
	Temperature	0	0

	Pressure	0	0
	Phase	supercritical	supercritical
	Density	0.30%	-3.21%
	gamma	4.29%	70.70%
	Viscosity	-1.23%	-53.62%
	Thermal conductivity	-2.81%	-38.04%

The thermodynamic models used are Sutherlands law for viscosity and thermal conductivity, with polynomial fits for specific heats per McBride *et al.*[3] with Richenberg's correction at high pressures[4]. The corrections are based on the ratio of the calculated pressure over the critical pressure. It is confirmed with Metacomp's help that the models are working correctly as implemented. However, these models underpredict transport properties for N_2, as found in the comparison with NIST data. Metacomp states that a literature will be conducted to seek better curve fits for a later release of CFD++. In the mean time, a decision was made to proceed with the simulations and analyses, keeping in mind the limitations of the thermodynamic properties near the critical point.

For checking convergence of CFD solutions, the histories of numerical residuals from the right hand side of the discretized governing equations are typically examined. For the water jet simulations, the numerical residuals of the final steady-state solution (used to initiate the time-accurate solutions) are three to four orders of magnitude below the maximum value, achieved after approximately 1000 iterations. For the supercritical simulations, the residuals of the final steady-state solution are on the same order of magnitude as the maximum value. The time steps in the time-accurate solutions are too small to significantly affect the convergence condition in the solutions. For instance, if a solution is not mass-balanced in the steady-state solution used as the initial condition, it would not be mass-balanced in the time-accurate calculations. Thus, the effort to achieve mass balance in the steady-state calculation became an integral part of the process to generate the time-accurate solution. Figure 15 shows the mass flow rate history at the outflow boundary of the dual-jet steady-state simulations. The runs require 7000-11000 iterations, with incremental decreases in the CFL number, in order to maintain a stable mass-balanced condition. The reason for the slow convergence may be grid related, choice of numerical parameters, or it may be due to the proximity to the critical point, where fluid properties change rapidly with variations in temperature. Although a rigorous grid-dependence study was not conducted due to the exploratory focus of this effort, an investigation is underway to identify the reason for the poor convergence in these calculations.

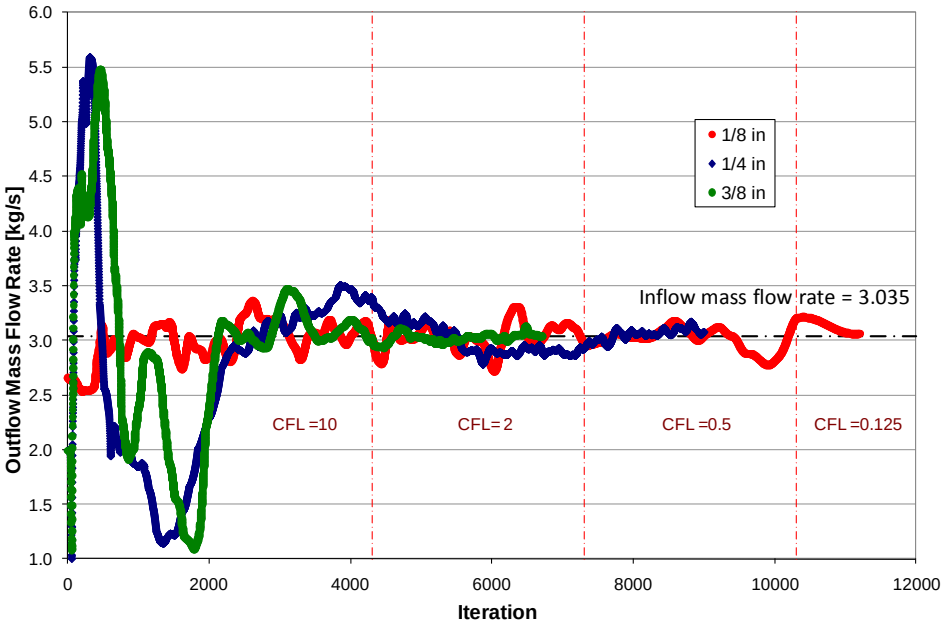

Figure 15: Mass Flow Rate History at the Outflow Boundary of Dual-Jet Simulations

SUMMARY

Project Themis is an in-house The cold flow phase of the research effort is intended as a preparatory and preliminary effort to gather more relevant data, increase confidence in modeling and simulation results and provide input to the relevant customer in a more reasonable timeframe. As previously stated a lack of scientific understanding has been identified by the Air Force Research Laboratory when it comes to the diluent injection/mixing configuration. There has been significant effort and research done in the simplified configuration known as jet-in-crossflow (JICF). Project Themis' intent is to build upon basic research done previously and investigate the flow physics in an applied research environment with simulative fluids, at similar conditions, with a relevant geometry, using water, cryogenic cold flow, and hot fire, experiments in conjunction with Computation modeling. Thus closing the gap between lab-scale basic research with large scale demonstration programs.

In support of design of the test apparatus in the Themis project experiment, CFD simulations are performed to provide insight into the behavior of water and supercritical jets injected transversely into a crossflow in a circular duct. Flow models incorporating Reynolds averaged Navier-Stokes are employed to provide insight into the behavior of interaction between the injected and freestream fluids, as well as between the jets themselves, at various momentum flux ratios.

Three sets of simulations are performed. First, water jet simulations are generated to validate CFD calculations against planar laser-induced fluorescence (PLIF) visualization results from water jet experiments performed for the Themis Project. Secondly, single jet cold flow simulations are conducted to identify supercritical jet behavior in a bounded crossflow and uncover technical issues in the modeling process. Finally, dual-jet cold flow simulations are performed to characterize jet interaction behavior at supercritical conditions.

The water jet simulations provide verification that the CFD calculations generate qualitatively similar results to the experiments. They also bring to light the fact that these flows are highly time-dependent, with large-scale fluctuations that enhance the diluent-freestream mixing.

The single jet simulations reveal the penetration behavior of the diluent jets with variations in the momentum flux ratios. The jet having the highest momentum flux ratio impinges upon the

opposite wall, breaking up the jet and inducing large-scale fluctuations in the flow, while lower momentum flux ratios generally maintain their coherence. It can be deduced that increases in momentum flux ratios increase the mixing between the diluents and the freestream.

The dual jet simulations reveal that the interaction between opposing jets have different characteristics depending on the momentum flux ratio. Quantitative assessments of the constituent mass fractions confirm the fact that higher momentum fluxes increase the diluents-freestream mixing in the dual jet configuration.

Modeling issues confronted in this study include the occasional tendency of the water jet simulations toward a pseudo-steady condition, the poor agreement of calculated thermophysical properties near the critical point, and slow convergence in the supercritical calculations. These challenges merit further investigation, which is underway as an ongoing effort.

ACKNOWLEDGEMENTS

The authors would like to acknowledge Lt. Michael Gorrilla, Farhad Davoudzadeh, and Allen Bishop from AFRL Edwards AFB for their technical contributions to this work. We are also grateful for the advice and guidance from Dr. Richard Cohn (AFRL) and David Peterson (Advatech).

This effort was sponsored through AFRL/ Applications and Assessment Branch (RZST), Contract Number FA9300-06-D-0003 Task Order 0008, with David Perkins and Franklin Friedl as Program Officers.

REFERENCES

1. CFD++ User Manual.
2. Menter, F.R. (1993), “Zonal Two Equation k-ω Turbulence Models for Aerodynamic Flows”, AIAA Paper 93-2906.
3. McBride, B. J, S. Heimel, S., Ehlers, J. G., and Gordon, S. "Thermodynamic Properties to 6000 K For 210 Substances Involving the First 18 Elements", NASA SP-3001, 1963.
4. Reid R.C., Prausnitz J.M., and Poling B.E., ***The Properties of Gases and Liquids***, 4th edition, 2nd print, McGraw-Hill, New York, 1988.
5. Sedano, N. et al. “Project Themis Update: ORSC cold-flow pre-burner experiment and modeling validation”, JANNAF 2010.
6. Thompson, R.A., Lee, K.P., Gupta, R.N. (1990), "Computer codes for the evaluation of thermodynamic properties, transport properties, and equilibrium constants of an 11-species air model", NASA TM-102602